River network rearrangements promote speciation in lowland Amazonian birds

Musher, Lukas J.

2022-04-08

Musher , L J , Giakoumis , M , Albert , J , Del-Rio , G , Rego , M , Thom , G , Aleixo , A , Ribas , C C , Brumfield , R T , Smith , B T & Cracraft , J 2022 , ' River network rearrangements promote speciation in lowland Amazonian birds ' , Science Advances , vol. 8 , no. 14 , 1099 . https://doi.org/10.1126/sciadv.abn1099

http://hdl.handle.net/10138/345764
https://doi.org/10.1126/sciadv.abn1099

DEVELOPMENTAL BIOLOGY

River network rearrangements promote speciation in lowland Amazonian birds

Lukas J. Musher[1,2]*, Melina Giakoumis[3,4], James Albert[5], Glaucia Del-Rio[6,7], Marco Rego[6,7], Gregory Thom[2], Alexandre Aleixo[8,9,10], Camila C. Ribas[11], Robb T. Brumfield[6,7], Brian Tilston Smith[2], Joel Cracraft[2]

Large Amazonian rivers impede dispersal for many species, but lowland river networks frequently rearrange, thereby altering the location and effectiveness of river barriers through time. These rearrangements may promote biotic diversification by facilitating episodic allopatry and secondary contact among populations. We sequenced genome-wide markers to evaluate the histories of divergence and introgression in six Amazonian avian species complexes. We first tested the assumption that rivers are barriers for these taxa and found that even relatively small rivers facilitate divergence. We then tested whether species diverged with gene flow and recovered reticulate histories for all species, including one potential case of hybrid speciation. Our results support the hypothesis that river rearrangements promote speciation and reveal that many rainforest taxa are micro-endemic, unrecognized, and thus threatened with imminent extinction. We propose that Amazonian hyper-diversity originates partly from fine-scale barrier displacement processes—including river dynamics—which allow small populations to differentiate and disperse into secondary contact.

INTRODUCTION

The lowland rainforests of the Amazon River basin are among the most diverse ecosystems on Earth, harboring more than 10% of all named species concentrated into an area that represents only about 0.5% of Earth's land surface area. Major hypotheses regarding the origins and assembly of this biota focus on the extreme heterogeneity of Amazonian environments, including the dendritic architecture of river drainage networks, the perennial role of river capture dynamics in fragmenting and merging riverine ecosystems through time and space, and the great antiquity of these systems dating back tens of millions of years (*1*, *2*). The riverine barrier hypothesis (RBH) posits that rivers can serve as barriers to dispersal and gene flow, fragmenting populations and causing diversification in many terrestrial organisms (*3*). Many rainforest assemblages of birds, primates, fishes, and other organisms exhibit high turnover in species composition on either side of large lowland Amazonian rivers (>1000-m width at low water; Strahler stream orders > 5), which dissect the whole region into broad interfluvial areas of endemism (*4*–*6*).

However, a burgeoning body of data indicates a more complex role for riverine barriers in generating patterns of Amazonian species richness. For example, comparative studies have shown that community-wide divergences across putative river barriers can be asynchronous (*7*), suggesting that divergence is instead driven by some combination of factors that include happenstance dispersal across preexisting barriers (*7*), environmentally mediated dispersal (*8*, *9*), and ecologically mediated divergence (*10*, *11*). Although the debate over barrier causality has often been framed in the context of dispersal versus vicariance (*12*), evaluating the RBH is complicated by the fact that barriers often change their location and permeability through geological time and across biogeographic space (*13*–*17*). Contemporary geographic features can therefore be poor indicators of past landscapes, a complication that has important consequences if trying to infer historical processes (*18*). For example, the river drainage network of lowland (below 250- to 300-m elevation) Amazonia is now understood to be highly dynamic, with mega-river capture events of more than 10,000 km^2 occurring on time scales of tens to hundreds of thousands of years (*19*, *20*). This dynamic landscape may be the primary mechanism generating patterns of aquatic biodiversity (*1*), but given such instability, some observers question whether Amazonian river courses actually persist long enough to act as effective barriers to gene flow for terrestrial organisms (*13*).

Despite much progress in understanding the processes mediating Amazonian diversification over time, a detailed picture of how biodiversity arises in this species-rich region is lacking. Most groups of Amazonian organisms lack genetic data with sufficient spatial resolution to discern the relationships between macroevolutionary processes (e.g., speciation and extinction) at biogeographic scales and microevolutionary processes (e.g., selection, migration, and drift) operating at populational scales (*21*, *22*). To that end, many studies have identified patterns of differentiation that occur between the major tributaries, rather than across them, including for birds (*23*–*26*), primates (*27*, *28*), squamates (*29*), and butterflies (*30*). These patterns of differentiation have sometimes been attributed to isolation by smaller rivers (100- to 1000-m width at low water) (*23*, *26*), but other environmental factors that might affect population structure have rarely been tested. Thus, if biodiversity arises at microgeographic scales, which fine-scale environmental features, if any, drive population differentiation, and do these features promote diversification via pure isolation or isolation with gene flow?

[1]Department of Ornithology, The Academy of Natural Sciences of Drexel University, Philadelphia, PA 19103, USA. [2]Department of Ornithology, American Museum of Natural History, New York, NY 10028, USA. [3]Department of Biology, City College of New York, New York, NY 10031, USA. [4]Graduate Center, City University of New York, New York, NY 10016, USA. [5]Department of Biology, University of Louisiana at Lafayette, Lafayette, LA 70503, USA. [6]Department of Biological Sciences, Louisiana State University, Baton Rouge, LA 70803, USA. [7]Museum of Natural Science, Louisiana State University, Baton Rouge, LA 70803, USA. [8]Finnish Museum of Natural History of Helsinki, University of Helsinki, Helsinki, Finland. [9]Museu Paraense Emílio Goeldi, Belém, Brazil. [10]Instituto Tecnológico Vale, Belém, Brazil. [11]Instituto Nacional de Pesquisas da Amazônia, INPA, Manaus, Brazil.
*Corresponding author. Email: ljm357@drexel.edu

The river capture hypothesis (RCH) posits that river network rearrangements (i.e., changes in riverine connections due to river captures and avulsions) that occur at appropriate spatial and temporal scales can drive diversification by increasing opportunities for speciation and dispersal and thereby reducing the probability of extinction (*1*). To test this hypothesis, the southern Amazon Basin offers a unique test case. Southern Amazonia is characterized by a marked topographical gradient, in which sediment-rich rivers originating in the Andes in the west meet upland (above the fall line ~250- to 300-m elevation; Fig. 1, map 2) rivers of the Brazilian Shield draining clearwater rivers from the southeast. These alternative geological settings, with rivers draining lowland sedimentary and upland-incising basins, tend to be more and less dynamic, respectively (*31*). Sediment-rich lowland rivers frequently rearrange and continuously change via tributary captures and avulsions (*32*). Sediment-poor shield rivers rearrange less frequently and are characterized by climatically or tectonically driven headwater captures and recaptures (*19*). These two topographical regimes meet within the Madeira-Tapajós interfluve, a region that has been a hot spot of Plio-Pleistocene diversification (*8*). Sediment-poor rivers in this region may rearrange at intermediate rates; their upstream portions flow over the Brazilian Shield where they are relatively stable, but downstream portions flow into the lowlands, where they become more dynamic (*19*). The Madeira-Tapajós also marks an ecotone in forest structure driven by varying climatic regimes, wherein humid rainforests are more densely vegetated in western Amazonia but transition into more open forests to the south and east (*33*, *34*). Given the many environmental gradients in Amazonia and its broad geographic extent, an important question is how river dynamics and environmental gradients influence demographic (e.g., gene flow) and phylogenetic (e.g., divergence and reticulation) histories in codistributed Amazonian organisms.

In this study, we sampled bird populations across the lowlands of southern Amazonia and sequenced hundreds of thousands of genetic markers to generate a dataset of 371 individuals sampled across six independently evolving species groups (table S1). These groups vary in the amount of phenotypic divergence from monotypic species with little variation (*Galbula cyanicollis* and *Malacoptila rufa*) to polytypic species (*Thamnophilus aethiops* and *Phlegopsis nigromaculata*) or species complexes (e.g., *Hypocnemis rondoni*, *Hypocnemis striata*, *Hypocnemis ochrogyna*, and *Hypocnemis peruviana* or *Willisornis poecilinotus* and *Willisornis vidua*) with considerable phenotypic and behavioral variation. Despite their differences, all these taxa share relatively limited dispersal capacities and are tied to upland forests, making them good subjects for studying the effects of river dynamics. Our objectives are to (i) characterize genome-wide levels of genetic diversity in codistributed avian species groups, (ii) test the drivers of population genomic divergence in each species group, (iii) quantify each species' history of differentiation and gene flow, and (iv) test the hypothesis that river rearrangements promote diversification and gene flow in Amazonian birds.

Assumptions, hypotheses, and predictions

Our hypotheses are predicated on a growing body of evidence suggesting that lowland Amazonian river networks are more dynamic over relatively short time scales of tens to hundreds of thousands of years than are upland (shield) rivers (*13*). Since river rearrangements represent both the genesis and elimination of barriers to dispersal and gene flow, events that occur at appropriate spatiotemporal scales may leave signatures in the diversification histories of taxa (*20*). Therefore, if upland rivers are barriers to terrestrial organisms, then rearrangements among these watercourses would have important populational and phylogenomic consequences. For example, frequent river rearrangements, such as those expected along lowland rivers of sedimentary basins, may hamper population differentiation by homogenizing allele frequencies among populations on either side of a river (*35*). On the other hand, rearrangements may promote diversification by facilitating secondary contact between populations that had previously diverged in allopatry, including, for example, cycles of isolation with infrequent introgression (i.e., reticulation) (*36*). Thus, if river dynamics inhibit diversification, then current river courses should not be strong predictors of population genomic structure because frequent rearrangements hamper divergence (*13*). Instead, other processes may be better predictors of genomic variation. For example, isolation by distance (IBD; in which genetic differentiation increases with increasing geographic distance) (*37*) and isolation by environment (IBE; in which genetic differentiation increases with increasing environmental disparity) (*38*) are deviations from panmixia that can mimic the population genetic predictions of isolation by barriers (i.e., allopatry). If riverine barriers do structure populations, then river-course rearrangements could stimulate diversification by promoting episodic isolation and secondary contact. In these cases, populations are not only expected to be structured across riverine barriers but also show evidence of varying degrees of gene flow or sympatry between differentiated populations.

RESULTS

Our analyses revealed fine-scale population structure and suggested a notable effect of modern river channels in structuring genetic diversity. We used restriction site–associated DNA sequencing (RADSeq) to sample genome-wide sequence data for six avian species groups codistributed across eight populations in the southern Amazonian lowlands and recovered high-quality sequences for all six species (Table 1). To visualize the geographic component of population structure, we defined these populations a priori as follows: (i) West Inambari: south of Solimões River and west of Purus River; (ii) East Inambari: Purus-Madeira interfluve; (iii) Rondonia 1: Jiparaná-Guaporé interfluve; (iv) Rondonia 2: Jiparaná-Roosevelt interfluve; (v) Rondonia 3: Roosevelt-Aripuanã interfluve; (vi) Rondonia 4: Aripuanã-Sucunduri interfluve; (vii) Rondonia 5: Sucunduri-Tapajós interfluve; and (viii) West Pará: Tapajós-Xingú interfluve (Fig. 1, map 1). These seven regions were selected for data visualization because they represent major interfluves bordered by rivers proposed to act as barriers (*23*–*26*).

After characterizing genomic diversity, we recovered population structure associated with river barriers in all six species (Fig. 1). To elucidate potential fine-scale patterns of differentiation in these taxa, we used *t*-distributed stochastic neighbor embedding (t-SNE), a machine learning dimensionality reduction algorithm that is capable of detecting subtle characteristics of datasets (*39*). Although t-SNE revealed similar results to a more commonly used principal components analysis (PCA; fig. S1), t-SNE recovered additional structure in *Willisornis* not detectable in the first two PC axes (Fig. 1). An independent method for assigning individuals to ancestral populations, STRUCTURE v2.3.4 (*40*), showed less geographic structuring overall but recapitulated the general pattern of rivers as barriers (Fig. 1 and fig. S2). In all analyses, a handful of individual

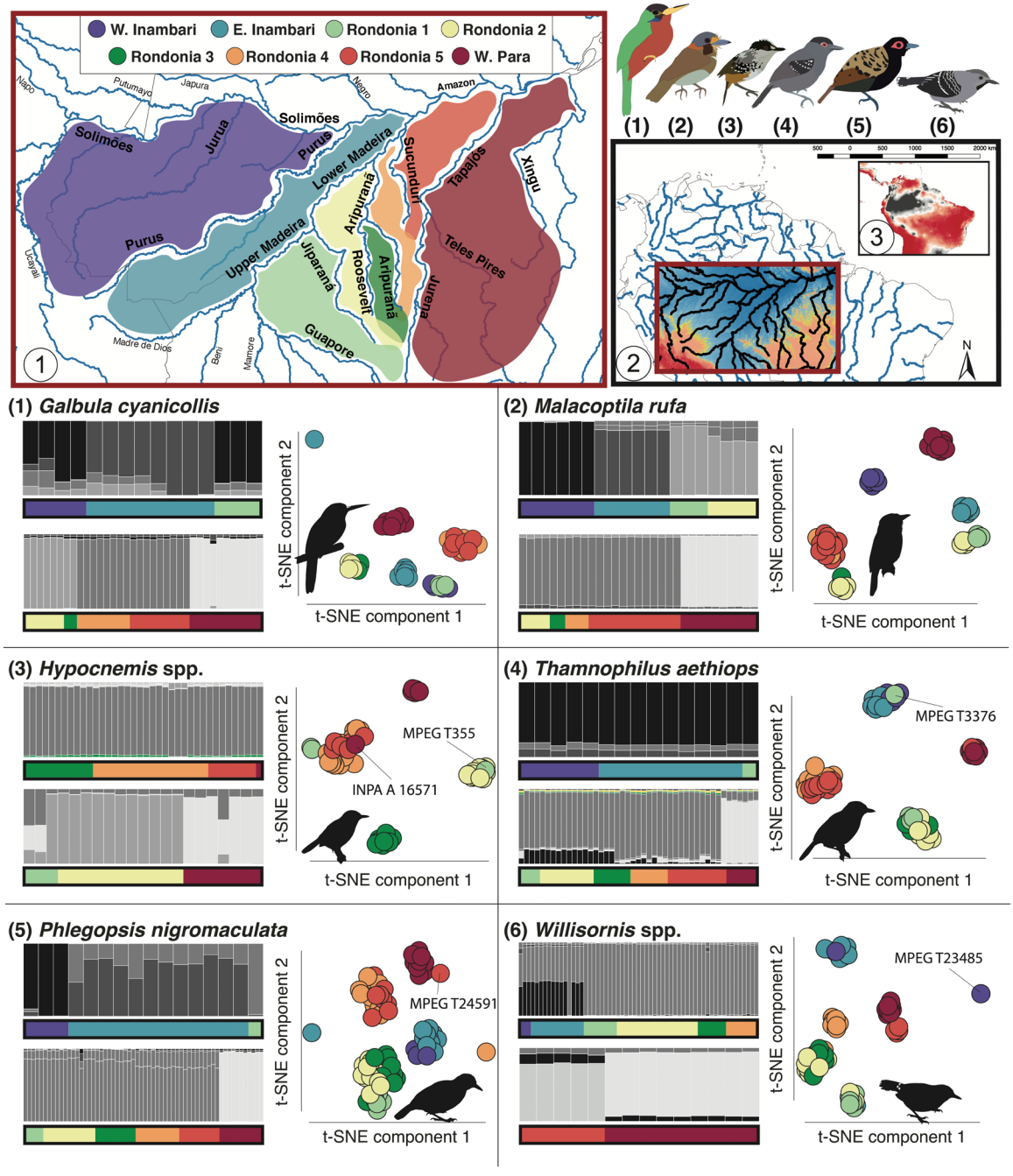

Fig. 1. Population genomic structure in six codistributed Amazonian bird species groups. For each species, results of the best *k* value for STRUCTURE analysis of split datasets (left) and example replicates of the *t*-distributed stochastic neighbor embedding (t-SNE) analysis (right) are shown. Colored bars underneath the STRUCTURE plots and circles on the t-SNE plots are colored on the basis of major interfluvial regions in map 1 (top left). Map 2 (top right) shows the topography of the study region within the dark red box, where yellow contours represent the 250- to 300-m elevational zone demarcating dynamic lowland (<250 m; shaded in blue) from relatively stable upland (>300 m; shaded in red) basins. Map 3 (top right inset) shows precipitation during the driest annual quarter (*76*), with high precipitation in gray, low precipitation in red, and a strong cline across the middle to lower reaches of the rivers draining the Brazilian Shield (plotted using QGIS).

samples clustered outside of their geographic populations, a pattern possibly indicating recent dispersal events.

Although all species were finely structured across space, we recovered unique spatial histories for each species group (Fig. 2). Species tree analyses (*41*) recovered robust phylogenetic topologies but differing area relationships among taxa. Bootstrap support for the relationships in these trees was generally high (>99), but the placement of the Rondonia 3 population in *Malacoptila* was unsupported. As the barrier associated with the deepest split in each taxon varied from large rivers such as the Madeira (*Hypocnemis* and *Phlegopsis*) and Tapajós (*Thamnophilus*) to smaller rivers such as the Aripuanã-Roosevelt (*Malacoptila*) or Sucunduri (*Willisornis*), these results

Table 1. Assembly statistics for all species groups. These statistics include the number of individuals in the assembly (*n*), the mean statistical depth of coverage, the SD of statistical depth of coverage, the number of loci in the assembly (total loci), the average number of loci per sample (mean loci), the range of loci per sample (range loci), and the species and citation of the reference genomes sampled.

Taxon	*n*	Mean coverage depth	SD coverage depth	Total loci	Mean loci	Range loci	Reference genome taxon	Genome citation
Galbula cyanicollis	53	25.92	7.19	87,606	46,669.10	13,585–60,141	*Galbula dea*	(*79*)
Malacoptila rufa	51	32.8	10.34	64,477	31,179.70	16,035–42,638	*Bucco capensis*	(*79*)
Thamnophilus aethiops	64	25.53	8.2	119,998	47,008.50	4,089–68,972	*Sakesphorus luctuosus*	(*79*)
Hypocnemis sp.	61	22.89	7.12	110,035	52,986.10	9,913–78,143	*Rhegmatorhina melanosticta*	(*80*)
Phlegopsis nigromaculata	77	24.5	6.4	122,081	64,081.80	19,603–83,765	*Rhegmatorhina melanosticta*	(*80*)
Willisornis sp.	83	23.46	5.54	143,810	64,410.70	14,266–81,671	*Rhegmatorhina melanosticta*	(*80*)

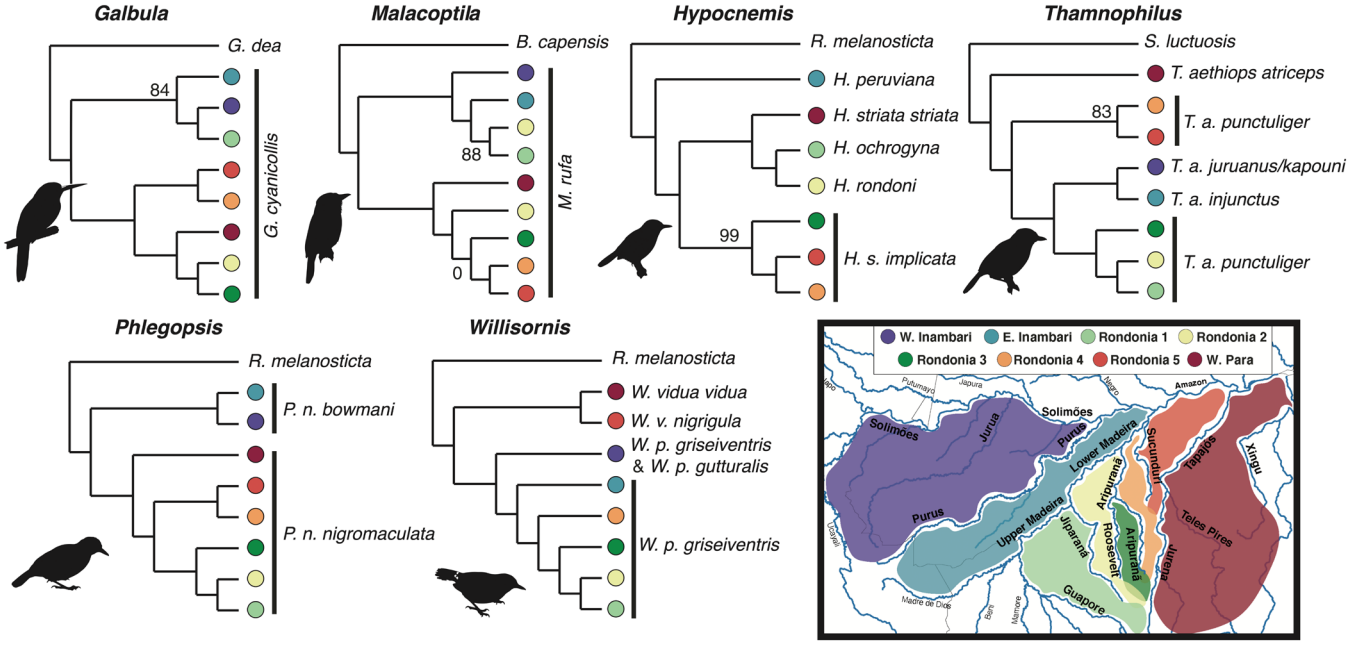

Fig. 2. Summary of phylogenomic results for six Amazonian bird species groups examined in this study. Results of species tree analysis in ASTRAL (*41*) showing the historical relationships among a priori defined populations in each species inferred from thousands of gene trees. All nodes are recovered with 100% bootstrap support except where noted.

support the hypothesis that rivers of various sizes are historically important for population divergence in these taxa across the central Amazon.

In *Malacoptila*, we identified two apparently reproductively isolated, secondarily sympatric populations in the Rondonia 2 area (Fig. 1 and figs. S1 and S2). These two overlapping populations were also syntopic, as they included two individuals, one from each population, collected at the same locality and date (MPEG T474 and MPEG T476). They are distantly related within this species group (Fig. 2), indicating secondary contact between divergent taxa despite strong isolation by barrier, a key prediction of the RCH.

Spatially explicit models of population connectivity and genetic diversity

We found that populations in dynamic regions west of the Madeira river and near to the mouth of the Tapajós River may have experienced higher rates of secondary contact (*42*). Whereas areas of low gene flow relative to expectations under pure IBD overlapped with riverine barriers, in contrast, gene flow tended to be higher west of the Madeira where rivers are most dynamic (Fig. 3 and fig. S3). In three groups (*Galbula*, *Phlegopsis*, and *Willisornis*), we recovered evidence of higher genetic diversity than expected under IBD west of the Madeira (Fig. 4 and fig. S4) despite high gene flow (Fig. 3 and

fig. S3), a pattern consistent with secondary contact. We also found evidence of high gene flow coupled with high genetic diversity west of the mouth of the Tapajós River and north of the Aripuanã River for *Hypocnemis* and *Thamnophilus*. Thus, populations in these dynamic regions were more likely to experience secondary contact, a result consistent with predictions of the RCH.

Predictors of genomic divergence

A multivariate logistic regression model incorporating geographic dispersal distance, environmental disparity, and rivers as predictors of genomic divergence (measured in pairwise Euclidean distances in t-SNE space) rejected the hypotheses of IBD and IBE as the primary drivers of divergences in all six groups. Specifically, we tested the assumption that the seven focal rivers were barriers and found that isolation by river was a significant predictor of genomic divergence in all groups irrespective of any nonindependence among predictor variables (Fig. 5 and Table 2) (*43*). The models strongly predicted genomic divergence in each species group (pseudo-R^2 = 0.30 to 0.74). Both rivers and dispersal distance were statistically significant predictors of divergence in each species group, but environmental disparity was often not significant (Table 2). Commonality analysis revealed that rivers were the most important predictor of genomic divergence in all six species groups, and their unique effects explained 31 to 60% of the total model fit. Although the unique effects of dispersal distance were relatively important for some species, explaining up to 13% of the model fit, dispersal distance was never as important of a predictor as rivers. The unique effect of environmental disparity, though, tended to explain very little of each model (0 to 5%). This result was relatively robust to coarser measures of genomic divergence and geographic distance (figs. S7 to S9 and tables S2 and S3). Thus, models explicitly testing the effects of IBD and IBE support the notion that rivers drive genomic divergence, a key prediction of the RBH and RCH.

Tests of introgression

Phylogenomic network analyses (*44*) recovered histories of introgression during diversification of these taxa despite clear spatial structuring around rivers, consistent with the RCH prediction that divergent populations experienced secondary contact (Fig. 6A). We specifically recovered two reticulation events—the maximum allowed in the analysis—in all species complexes but one (*Willisornis*). In most species, the most credible network topology was highly supported [posterior probability (PP) = 1.0], but the best models for *Malacoptila* and *Thamnophilus* were less supported. Still, alternative topologies for these two species recapitulated similar patterns of reticulation (fig. S10). Unlike in other species, the dominant network topologies for *Hypocnemis* and *Thamnophilus* groups were inconsistent with the results of the species tree analysis, which suggests that ancestral gene flow among differentiating populations has obscured species tree inference for these taxa. Estimates of interpopulation gene flow using a maximum likelihood population graph (*45*) were mostly consistent with the network modeling results, although with some notable differences (Fig. 6B). The best-fitting population graph model included at least one admixture edge

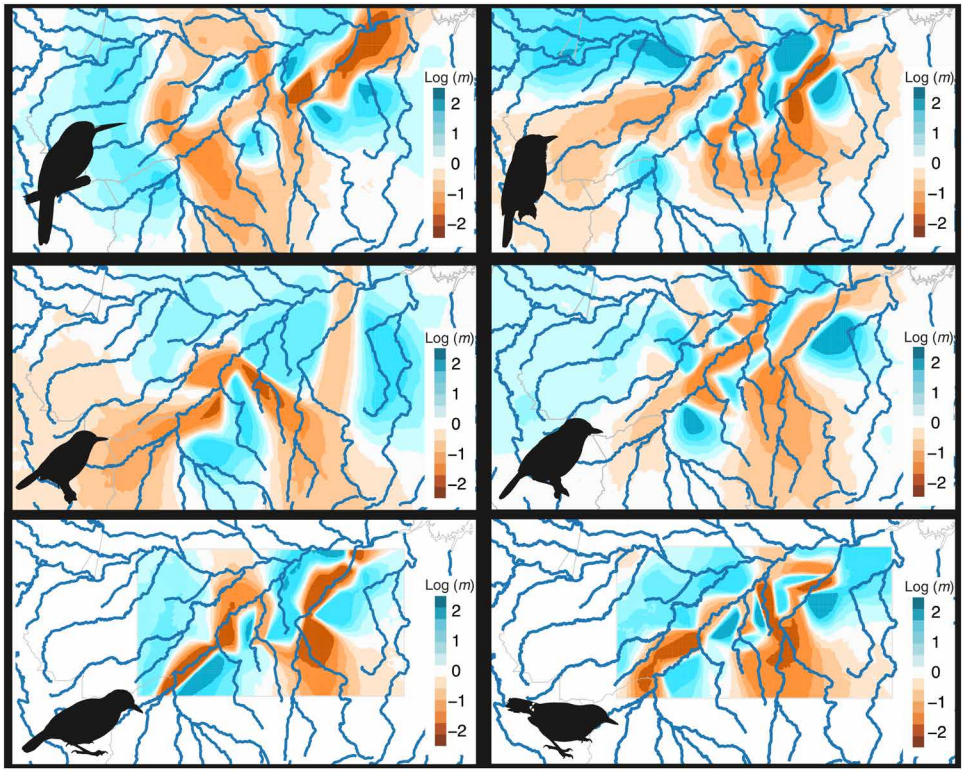

Fig. 3. Effective migration (gene flow) results estimated in EEMS. Results are shown for (left to right and top to bottom) *G. cyanicollis*, *M. rufa*, *Hypocnemis* spp., *T. aethiops*, *P. nigromaculata*, and *Willisornis* spp. Effective migration rate (*m*)—a measure of gene flow—is shown on a $\log_{10}$ scale relative to the expected value under an IBD model across the sampled range. Darker blues correspond to higher effective migration rate, whereas darker oranges correspond to lower rates.

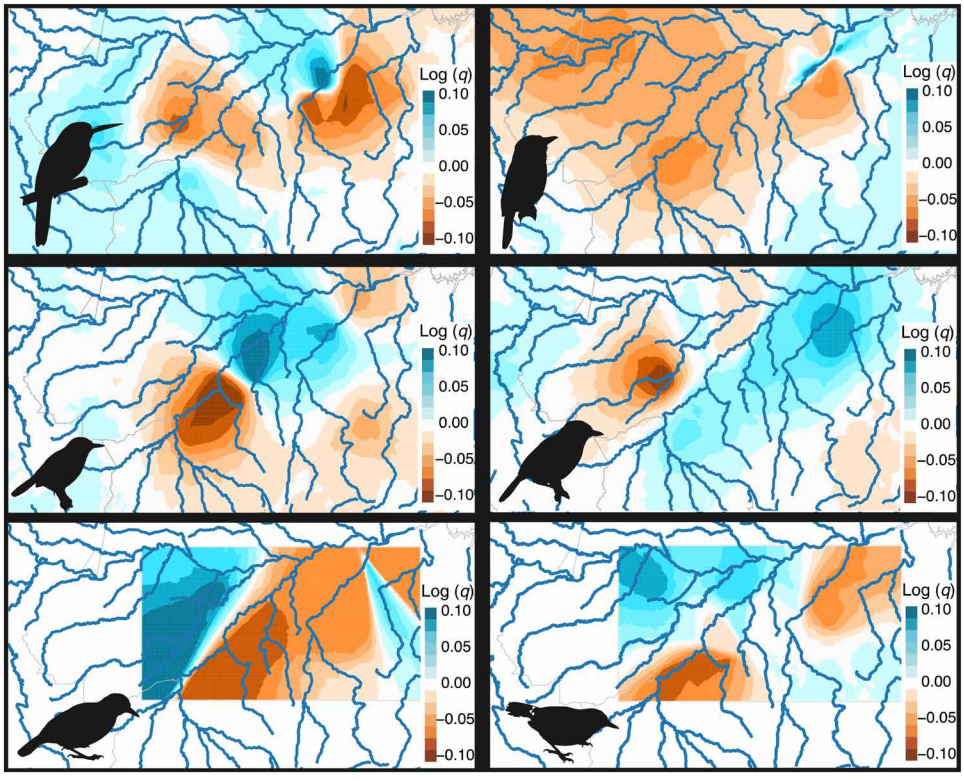

Fig. 4. Effective diversity (dissimilarity) results estimated in EEMS. Results are shown for (left to right and top to bottom) *G. cyanicollis*, *M. rufa*, *Hypocnemis* spp., *T. aethiops*, *P. nigromaculata*, and *Willisornis* spp. Effective diversity (*q*) is shown on a $\log_{10}$ scale relative to the expected value under an IBD model across the sampled range. Darker blues correspond to higher genetic diversity (dissimilarity), whereas darker oranges correspond to lower diversity.

in each species but with diminishing gains in likelihood after that (Fig. 6C). Thus, many adjacent populations separated by rivers likely experienced substantial post-isolation gene flow.

Our analyses also revealed evidence of lineage fusions, implying that portions of divergent populations have merged in the past. Within multiple species, at least one daughter node was recovered, showing nearly equivalent inheritance probabilities from each of two parent nodes (*Galbula*, *Hypocnemis*, and *Thamnophilus*), where inheritance probability represents the proportion of sampled genes inherited through gene flow (Fig. 6A). For example, the genome of *H. ochrogyna*, a phenotypically and behaviorally distinct taxon, resulted from nearly equivalent inheritance probabilities of parent nodes of different taxa, *H. striata* ($P = 0.49$) and *H. peruviana* ($P = 0.51$), a scenario theoretically consistent with hybrid speciation (*46*). Similarly, *Thamnophilus aethiops punctuliger* has nearly equal shared ancestries with taxa in East and West Inambari (*Thamnophilus aethiops kapouni*, *Thamnophilus aethiops juruanus*, and *Thamnophilus aethiops injunctus*) and Pará (*Thamnophilus aethiops atriceps*). Within *G. cyanicollis*, multiple reticulate (nonbifurcating) nodes with high inheritance probabilities were associated with populations isolated by the Madeira and Purus, rivers known to have rearranged historically (*13*). Because incomplete lineage sorting is theoretically accounted for in the multispecies network coalescent (MSNC) model, these shared ancestries are presumably driven by introgression. Thus, we reveal an additional potential outcome of certain river network rearrangements, lineage fusion that results in genetically distinct lineages from the introgressing populations.

Demographic modeling

Demographic modeling of divergence times (while accounting for gene flow among populations) (*47*) revealed that all divergences likely occurred within the past 2 million years and that all extant populations were <1 million year (Ma) old (fig. S11). However, divergences across the same river were asynchronous. Splits across the Tapajós varied, possibly forming two general groups: one at about 700 thousand years (ka) ago to 1 Ma ago and another at about 300 ka ago (fig. S11B). Splits across the Madeira also varied, with most divergences being <1 Ma ago (fig. S11C). Across the Aripuanã-Roosevelt basin, divergences were mostly between 250 and 500 ka ago, except for *Phlegopsis*, which occurred about 70 ka ago (fig. S11D). Although only three of the groups were differentiated across the Purus, two of these (*Galbula* and *Malacoptila*) diverged about 300 ka ago (fig. S11E). Relative rates of gene flow based on these models were consistent with previous analyses (table S5). In all species with gene flow across the upper Madeira (*Galbula*, *Hypocnemis*, *Thamnophilus*, and *Phlegopsis*), the rate of gene flow was asymmetrical; it was often substantially higher from east to west than from west to east in forward time, with little overlap in 95% credible intervals.

DISCUSSION

We demonstrated that the spatial distributions of genomically characterized lineages within six Amazonian bird clades (i.e., species groups) that inhabit terra firme (nonfloodplain) rainforests in southern Amazonia are delimited by the current position of many

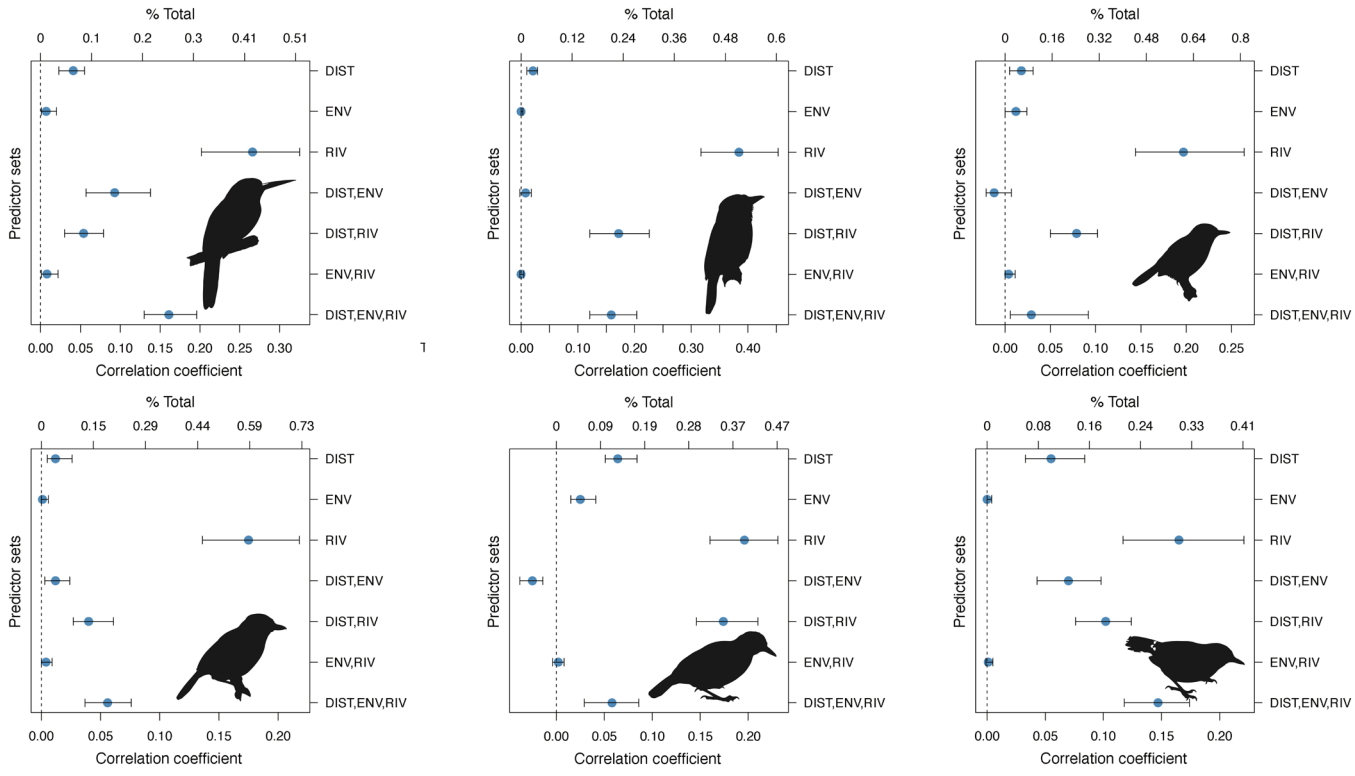

Fig. 5. Rivers are the most important predictors of genomic divergence. The plots show the results of the variance partitioning (commonality analysis) of the multivariate logistic regression model, $D \sim \text{DIST} + \text{ENV} + \text{RIV}$, where D is the pairwise genomic divergences across t-SNE space, DIST is the dispersal distance, ENV is the environmental disparity, and RIV is the separation by rivers. The commonality coefficients of seven predictors (three unique and four common) for each species represent the proportion of variance of pairwise genomic divergence among samples that are explained by each predictor or set of predictors. The percent total represents the proportion of variance explained by the overall multivariate model that is explained by each predictor or set of predictors. Confidence intervals of 95% around each value were computed using 1000 bootstrap replicates with subsampling of 90% of samples. The order of species is (from left to right beginning at the top) *Galbula*, *Malacoptila*, *Hypocnemis*, *Thamnophilus*, *Phlegopsis*, and *Willisornis*. Exact values for these parameters can be obtained in Table 2.

rivers, each with distinct hydrological and geomorphological profiles. Because existing river courses are the primary predictors of genomic divergence patterns in these species groups (*7*), our findings support the hypothesis that river dynamics promote diversification in southern Amazonia. Moreover, the phylogenetic histories of these taxa are spatially incongruent, and the divergence times across focal rivers are asynchronous, indicating that a simple model of river formation (i.e., one river and one vicariant event) alone cannot explain patterns of divergence. Instead, our results suggest that a substantial portion of Amazonian biodiversity may be a product of historical barrier instability and dynamism across multiple scales.

Here, we reveal that establishing secondary sympatry has had several distinct biological outcomes, including coexistence (*Malacoptila*), introgression (most groups), and possibly hybrid speciation (*Hypocnemis*) (*48*). For example, we show that *M. rufa* experienced limited gene flow among differentiated populations, but secondarily sympatric populations in the Rondonia 2 area remained differentiated, indicating that these two populations are reproductively isolated. In other species, populations remained differentiated across rivers despite significant introgression from nonsister lineages (e.g., *Galbula*, *Thamnophilus*, and *Phlegopsis*). We even found one potential incidence of homoploid hybrid speciation, wherein *H. ochrogyna*—a widely recognized biological species (*25*)—might have resulted from an ancestral fusion between populations of *H. peruviana* and *H. striata*. Together, these results expose the necessity of accounting for gene flow when estimating evolutionary relationships in Amazonian taxa (*49*).

Homoploid hybrid speciation is thought to be rare in vertebrates, but recent studies have highlighted an increasing number of examples (*46*, *50*). Lineage fusions, wherein diverging lineages—or portions of those lineages—merge to become geographically isolated but admixed evolutionary entities, seem to be more common than previously realized (*51*, *52*). These fusions have been proposed to occur due to a number of biogeographic mechanisms that include river rearrangements in Amazonia (*46*). The examples identified here imply that the disappearance of physical barriers to gene flow can facilitate the merging of divergent populations, which may then emerge as novel admixed taxa (*53*). However, further work is needed to confirm whether the reticulate examples we identify are truly the examples of hybrid speciation or some other mechanism.

Bridging diversification models of aquatic and terrestrial Amazonian organisms

Spatiotemporal patterns of biodiversity are shaped by geophysically and climatically generated cycles of fission and fusion among populations, species, and biogeographic areas (*54*). These episodic cycles play out across multiple scales across the globe as ecosystems expand and contract, barriers to dispersal wax and wane, and as

Table 2. Results of the multivariate logistic regression and additional parameters of the commonality analysis. Model fit index (pseudo-R^2), beta weights (β), odd ratios (Ψ), *P* values (*P*; ***$P < 0.001$), and the unique (*U*), common (*C*), and total contributions of each predictor to the variance in dependent variable and the percent of the model fit explained by each. Percent contributions to the model are shown in parentheses. Rows in boldface font highlight the statistically significant predictor with the highest total contribution to the variance in genomic divergence.

Species	Pseudo-R^2	Predictor	β	Ψ	*P*	*U*	*U* (%)	*C*	*C* (%)	Total	Total (%)
Galbula	0.63	DIST	0.27	1.31	***	0.04	6.50	0.31	48.94	0.35	55.44
		ENV	0.07	1.08	0.003	0.01	1.17	0.26	41.62	0.27	42.79
		RIV	**0.23**	**1.26**	***	**0.27**	**42.16**	**0.22**	**35.44**	**0.49**	**77.60**
Malacoptila	0.74	DIST	0.19	1.21	***	0.02	2.77	0.34	45.54	0.36	48.31
		ENV	−0.01	0.99	0.745	0.00	0.01	0.17	22.44	0.17	22.45
		RIV	**0.23**	**1.26**	***	**0.38**	**51.67**	**0.33**	**44.52**	**0.72**	**96.19**
Hypocnemis	0.33	DIST	0.10	1.11	***	0.02	5.61	0.10	29.46	0.12	35.07
		ENV	−0.07	0.94	***	0.01	3.68	0.02	6.63	0.03	10.31
		RIV	**0.14**	**1.15**	***	**0.20**	**59.97**	**0.11**	**34.30**	**0.31**	**94.27**
Thamnophilus	0.30	DIST	0.07	1.07	***	0.01	4.04	0.11	36.12	0.12	40.16
		ENV	0.02	1.02	0.191	0.00	0.38	0.07	23.85	0.07	24.23
		RIV	**0.16**	**1.17**	***	**0.17**	**58.25**	**0.10**	**33.29**	**0.27**	**91.54**
Phlegopsis	0.49	DIST	0.18	1.19	***	0.06	12.97	0.21	42.05	0.27	55.02
		ENV	−0.06	0.94	***	0.02	5.00	0.04	7.14	0.06	12.14
		RIV	**0.10**	**1.10**	***	**0.20**	**39.65**	**0.23**	**47.37**	**0.43**	**87.02**
Willisornis	0.54	DIST	0.25	1.29	***	0.05	10.09	0.32	59.08	0.37	69.17
		ENV	−0.01	0.99	0.581	0.00	0.02	0.22	40.38	0.22	40.40
		RIV	**0.13**	**1.14**	***	**0.17**	**30.55**	**0.25**	**46.45**	**0.42**	**77.00**

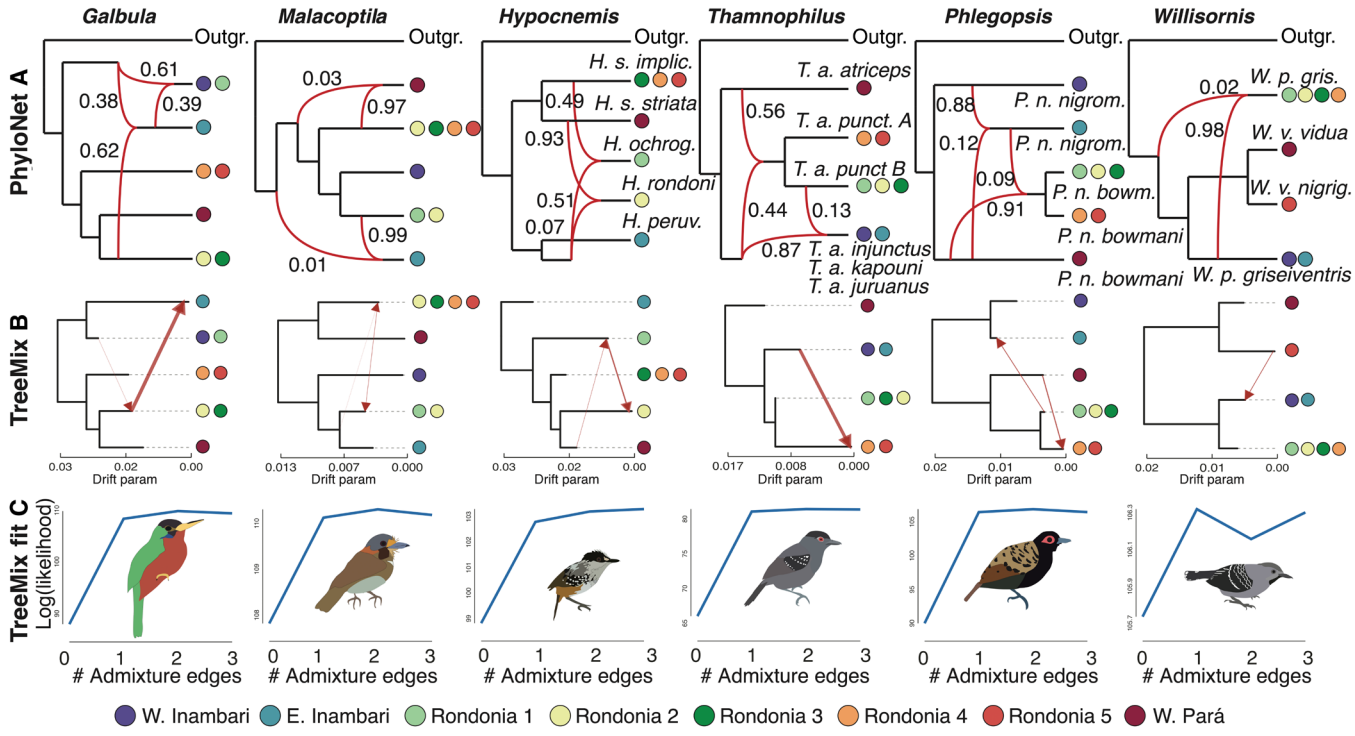

Fig. 6. Summary of phylogenomic network results for six Amazonian bird species groups examined in this study. (**A**) Results of Bayesian network analysis in PhyloNet (*44*) showing the most credible topology for each species group. Reticulate branches are shown in red and labeled with inheritance probabilities. Tips are labeled with taxonomic designations for all polytypic species groups. (**B**) Results from TreeMix showing the inferred topology among populations (black branches) and inferred admixture edges (red arrows). The thickness of each migration edge is proportional to its inferred magnitude. (**C**) Results of the model-fitting exercise in TreeMix. The *y* axes show the average log(likelihood) among all TreeMix replicates that varied in missing data thresholds for each value of *m* (the number of admixture edges). Circles at the tips of all networks are colored on the basis of a priori defined populations (Fig. 1, map 1). Because PhyloNet and TreeMix populations were assigned using the results from STRUCTURE (*45*), multiple a priori defined populations may be sampled in a given tip.

biotic dispersal drives distributional change over time (*11*, *15*, *55*, *56*). At shallow evolutionary time scales, and as exemplified here, these fission-fusion cycles can generate diversity by driving differentiation via isolation, colonization, and introgression (*36*, *51*).

Our study exemplifies one possible geomorphological mechanism—river drainage evolution and rearrangement—through which these fission-fusion cycles may play out for Amazonian organisms that rarely cross rivers and their associated floodplains (*57*). This mechanism is already thought to have had a profound effect on freshwater fish diversity, which reaches its global zenith in lowland Amazonia, but has rarely been studied for terrestrial organisms (*6*). For example, fish alpha diversity (local diversity) is highest at Amazonia's core, in the lowland sedimentary basins, where the low topographic relief facilitates frequent connections and disconnections among watersheds driven primarily by erosional forces. In contrast, fish beta diversity (endemism) is higher in the upland shields at Amazonia's periphery, where rearrangements occur less frequently (*5*). To summarize, more frequent river rearrangement is thought to facilitate higher rates of both isolation and dispersal (i.e., secondary contact) among adjacent watersheds, thereby promoting low spatial and high temporal fish species turnover in lowland western Amazonia (Amazonia's core). Slower rearrangements, though result in high spatial and low temporal turnover in the upland portions of eastern Amazonia (Amazonia's periphery) (*1*).

This core-periphery pattern is mirrored by broad patterns of many terrestrial organisms in two ways. First, phylogenetically underdispersed communities of birds inhabiting the tectonically unstable western basin indicate rapid in situ diversification and the repeated establishment of secondary sympatry, while phylogenetically overdispersed communities of the more stable Brazilian Shield suggest slower diversification with higher local endemism (*12*, *31*). Second, rate estimates of phylogeographic lineage splitting for Amazonian birds are higher in the western lowlands than eastern shields. Rates of lineage loss, however, are overall higher in the uplands (*21*). Our results show that this pattern holds true for certain taxa at microevolutionary scales as well; effective diversity is higher across western Amazonia for three of the six taxa despite higher rates of migration, implying more rapid episodes of isolation and secondary contact at the epicenter of drainage rearrangement (Figs. 3 and 4 and figs. S3 and S4). Our data also lend support to this model in another important way: We show that the biogeographic processes acting on Amazonian birds at this intermediate scale are dominated by isolation by barrier and not local adaptation to environmental differences, as environmental disparity explains little, if any, variation in genomic divergence for all sampled taxa (Fig. 5 and Table 2).

Through this study, we may catch a glimpse of how barrier displacement in the form of river rearrangement can facilitate isolation and secondary contact as populations of *M. rufa* in the Rondonia 2 area became syntopic and others show reticulation. For example, although no two species' histories were phylogenetically congruent with respect to the details of geography, some general patterns emerged among species groups. All six groups showed either phylogenetic

(*Galbula*, *Malacoptila*, *Thamnophilus*, and *Willisornis* species trees) or reticulate (*Galbula*, *Malacoptila*, *Hypocnemis*, and *Thamnophilus* networks) affinities across the upper Madeira, a section of river thought to have been captured from a tributary of the Purus during the late Quaternary (Figs. 2 and 6) (*13*). Demographic modeling recovered asymmetric gene flow (stronger from east to west) for all species that experienced gene flow across this barrier (table S5), which is consistent with such an eastward shift in that river. Taken at face value, our data suggest that this capture event occurred roughly 100 to 800 ka ago, consistent with or older than previous estimates (fig. S11C) (*13*, *58*). Similarly, five of six species showed phylogenetic or reticulate affinities across the lower Tapajós, where avulsion shifted the mouth of the main channel multiple times (*19*). Phylogenomic trees and networks show that the Pará population is sister to northern populations of the Madeira-Tapajós for *Malacoptila* (Rondonia 2 to 5) and *Willisornis* (Rondonia 5), implying that these avulsions at the mouth of the Tapajós may have occurred during the late Quaternary (fig. S11B), which is consistent with the geological literature (*19*). Moreover, in *Galbula* and *Hypocnemis*, the Pará population is sister to populations at the center of the Madeira-Tapajós (Rondonia 2 and 3), where river capture is thought to have shifted drainage from Madeira tributaries to Tapajós basins (*5*). Overall, then, we provide evidence that drainage instability, rather than river formation sensu stricto, may contribute to diversification dynamics in many Neotropical organisms limited by rivers.

Therefore, the RCH as a general framework unifies the biogeographic theory of both aquatic (primarily freshwater fish) and terrestrial (primarily birds and primates) Amazonian vertebrates and implies a common cause for species accumulation in these groups (*31*). First, macroevolutionary patterns of biodiversity seem to arise at microevolutionary scales (*21*–*23*, *26*, *28*), and here, we demonstrated that even small rivers can be key drivers of microevolutionary diversity for many Amazonian birds (Fig. 5 and Table 2). Since lowland rivers are typically dynamic, we propose that, like many aquatic organisms, Amazonian terrestrial diversity originates from river dynamics at local to regional scales, which promote the early divergence of populations, forming spatially restricted and differentiated populations (i.e., taxa) (*20*). Ongoing river rearrangements may then promote dispersal, leading to secondary contact among previously isolated populations, as well as subsequent isolation and divergences. As these rivers shift course via river capture and avulsion, they directly affect the three fundamental parameters of diversification: dispersal (colonization after the loss of barriers), speciation (via isolation and secondary contact), and, theoretically, extinction (via changes to population connectivity or spatial restriction) (*1*). Given Amazonia's ancient history and probable low extinction rates (*21*), we propose that the repetition of this process through deep time may have promoted the accumulation of a large portion of its vertebrate diversity. If so, Amazonia would be both a species pump that continuously generates new diversity and a "museum" for old lineages that originated in or colonized the South American tropics long ago (*59*, *60*).

Broader implications: The drivers of Amazonian endemism

From a broader perspective, our results suggest that a long-recognized area of endemism [Rondonia sensu Cracraft (*4*); i.e., the Madeira-Tapajós interfluve] may not represent a historically unified biogeographic area for many taxa. In four of the six sampled species groups, sets of populations within Rondonia were not reciprocally monophyletic. Rather, *Galbula*, *Malacoptila*, *Hypocnemis*, and *Willisornis* all included lineages within Rondonia with sister relationships either west of the Madeira or east of the Tapajos, rather than to other Rondonian populations. Previous work similarly demonstrated nonreciprocal monophyly of populations within Rondonia in addition to fine-scale landscape partitioning of phylogeographic lineages within this region (*26*). Our results support this observation, as we elucidate fine-scale co-occurrent distributions of phylogeographic lineages of Amazonian birds that largely overlap with those of other studies (*23*, *24*, *26*, *61*). The patterns and processes that we identified are likely not limited to the region's avifauna; the distributions of primates in Rondonia are notably similar to, if not more spatially restricted than, those identified here (*62*, *63*). Thus, the Rondonia area of endemism, although descriptive at one spatial scale, can be deconstructed when assessing patterns at finer scales.

Consequently, we suggest that areas of endemism in general may be described on the basis of a misconstrued understanding of patterns of biodiversity. As we show, the histories of species in this study were characterized by gene flow among nonsister taxa (genomic reticulation) and exhibit phylogenetic incongruence with respect to the details of geography (biogeographic area reticulation) (*5*). Indeed, the biota of all areas of endemism may be assembled by a reticulated phylogenetic history of dispersal, in situ speciation, and local extirpation (*7*, *64*). Thus, portions of Rondonia have been connected to and disconnected from other areas over evolutionary time, and as a result, the components of its biota are of different ages (*5*, *7*). Although Rondonia contains a distinct contemporary biological community that is unequivocally real at a coarse spatial scale, this observation may be biogeographically misleading as it is in part a construct of taxonomic artifact (unrecognized taxa at smaller spatial scales) and in part the result of multiple superimposed histories of isolation and expansion yielding quasi-congruent spatial patterns (*64*).

In general, then, we propose that areas of endemism may instead result because taxa originate at smaller scales and then expand their ranges as dynamic barriers to dispersal erode. In regions with high rates of river rearrangement such as the western Amazon, the signal of fine-scale diversification and endemism may quickly dissipate because of high temporal turnover of taxa (*12*, *31*). In regions with somewhat slower rates of displacement, such as those within the Madeira and Tapajós basins, where upland shield and lowland sedimentary rivers meet, the signal of local diversification may persist over longer time periods, facilitating detection by studies such as ours (*12*, *26*). Therefore, as Amazonian watersheds are reticulate biogeographic areas for obligate aquatic and riparian organisms (*5*), so too might they be for endemism in some birds.

Previous work has shown that avian population differentiation may occur more than three times faster than speciation in the Neotropics, which implies that many differentiated populations (i.e., young, spatially restricted taxa like those identified here) are short-lived (*22*). Thus, we argue that fine-scale ephemeral processes, such as river rearrangement, may aid in generating diversity, but this diversity eventually expands to reach barriers that are, although not static in the strict sense, less permeable at a given point in time (*31*). These dynamics may often, but not always, result in sister relationships across larger rivers over deeper time scales of millions of years (*65*).

Limitations and future directions

Although our findings support the RCH, the effects of rivers likely interact with other processes. For example, climate change can alter

the strength of riverine barriers and can also drive local extinction dynamics, thereby mediating extinction-recolonization cycles (*8*). Such effects of climate on barrier effectiveness may be difficult to distinguish from river rearrangements in the strict sense based on the data we provide and could also explain some patterns found here. Given that there are many young divergences across the Brazilian Shield (*8*), future work should directly compare processes occurring in lowland and upland basins across Amazonia to disentangle the two processes with more certainty (*1*).

Furthermore, the occurrence of rare but consequential (i.e., sweepstakes) dispersal events across rivers—thought to be rare in many understory taxa (*57*)—may be difficult to distinguish from a barrier displacement model in practice. Future work explicitly testing pulse migration versus continuous migration models of gene flow may help clarify the relative contributions of these two nonmutually exclusive mechanisms. Nevertheless, the explicit assumption of the framework presented here is that the underlying lowland riverine landscape is not stable, which has also been confirmed, for instance, on the easternmost Amazonian part of the Brazilian Shield (*66*, *67*). Within this conceptual framework, drainage network evolution is a simple solution to the question of how secondary contact occurs between differentiated taxa that are otherwise isolated by rivers.

Historically, many biogeographic models have treated organisms as passive participants in biotic diversification, where the landscape alone dictates dispersal dynamics and rates of gene flow (*68*). Although our model highlights the profound effects of Earth history processes underlying the evolutionary processes of speciation and gene flow, it does not preclude the unquestionable influence of other mechanisms in contributing to such diversity patterns (*10*, *11*). For example, much of previous work has shown that dispersal capacity (vagility) has a measurable impact on divergence rates (*11*). In this study, however, we focus on avian taxa that have a relatively weak propensity to dispersal with the goal of testing whether and how river dynamics contribute to diversification in these terrestrial organisms. Although we argue that the RCH explains a substantial portion of the patterns observed, the patterns and processes of biotic diversification are better understood as layered, with dispersal and local extinction affected by organismal traits contributing to persistence on the landscape (*7*). Therefore, future work should assess how the RCH interacts with other mechanisms that influence speciation, persistence, and adaptation, in addition to how this process plays out for other, more dispersive groups of birds.

The future of Amazonian biodiversity

Amazonian biodiversity is unmatched by any other terrestrial ecosystem (*69*). Still, we demonstrate that its species richness may be greatly underestimated even in well-studied groups such as birds (*2*, *70*). This diversity, though, is nonrandomly distributed across the basin, with community composition shifting across many rivers (*4*, *12*). Our results corroborate those of other studies that have reported fine-scale patterns of diversity across the Madeira-Tapajós interfluve—a region threatened by rapid and ongoing deforestation (*26*, *71*)—yet this diversity is generally unrecognized (*69*). Many of the populations delimited by these rivers represent taxa, as they are differentiated, isolated evolutionary entities even if they are genomically admixed. They are relatively young (<500 ka) and spatially restricted. That these taxa are micro-endemic conveys the severity of future biodiversity loss in southern Amazonia should deforestation continue at current levels (*72*, *73*); that many of them are not yet named and formally described reveals how much fundamental biological information of the Amazonian avifauna is threatened with loss to imminent extinction.

MATERIALS AND METHODS

Restriction site–associated DNA sequencing

We extracted total DNA from vouchered fresh tissue samples using a DNeasy tissue extraction kit (Qiagen, Valencia, California), which recovered sufficiently high-quality DNA (>10-kb fragments) for all samples. Library prep for RADSeq was then performed at the University of Wisconsin Biotechnology Center (Madison, WI) using two enzymes (Pst l and Msp l) but barcoding only a single cut site (TGCA). We then performed 150–base pair (bp) paired-end sequencing on an Illumina NovaSeq.

Raw Illumina reads were processed using iPyrad version 0.9 (*74*). We first demultiplexed the raw reads and trimmed low-quality base pairs and then aligned reads for each species to a reference genome. We specifically applied a minimum coverage for statistical base calling of six, with a minimum trimmed read length of 35 bp, a maximum of 5% uncalled bases and 5% heterozygous sites, and a mapping threshold of 0.9. These steps were repeated to generate variant call format files for each species group, which were used and filtered for downstream analyses.

Characterization of genomic variation

We took multiple approaches to characterize genomic diversity across each species without a priori geographic bias. First, we used iPyrad API analysis tools (*74*) to perform PCA on unlinked (one randomly sampled genotype per locus) genotype calls for each species group. Because RADSeq datasets often contain a large proportion of missing data, we performed PCA after imputing missing genotypes based on population assignments in *k*-means clustering implemented in the iPyrad API. This method allows imputation without a priori bias about population assignments (the eight a priori areas were chosen only for data visualization; the assumption of rivers as barriers was tested using multiple approaches). Specifically, we assumed $k = 8$ for all species (except *Hypocnemis* because West Inambari was not sampled) and used iterative clustering to group individuals into populations. For iterative clustering, we first sampled single-nucleotide polymorphisms (SNPs) present across 90% of individuals in the assembly and then clustered with the assumed *K*. This was repeated five times, allowing more missing data at each successive iteration until reaching a minimum of 75% coverage at each sampled SNP. Although *k*-means clustering is a crude method for population assignment, it is used only to minimize geographic bias during imputation and thus to reduce bias in downstream analyses. To impute, we randomly sampled genotypes based on the frequency of alleles within each of the populations defined by *k*-means. We then used t-SNE to decompose the PCA results into fewer dimensions, which is explained in further detail below. PCA and t-SNE are dimensionality reduction tools and do not test hypotheses on their own.

Spatially explicit models of population connectivity and diversity

To examine how the distribution of population genomic diversity within each species group varies across space, identify regions of high or low dispersal, and evaluate the contribution of IBD to spatial patterns of genetic variation, we used estimated effective migration surfaces (EEMS) (*24*). As input for EEMS, we first computed

pairwise genetic distance matrices (d_{xy}) between individuals for each species complex using iPyrad API analysis tools (*74*). To generate polygons to constrain the spatial extent of the analysis, we drew a rectangle around all sampled localities for each species and distributed 1000 demes over each one. We then performed three runs of the Markov Chain Monte Carlo (MCMC) for 2,000,000 iterations, thinning every 10,000 iterations, and excluded a burn-in of 1,000,000 iterations. The convergence of the MCMC was visually assessed by plotting the log PPs of each run and comparing results among runs for the same species. When results were converged among runs, a single run was chosen.

Testing the predictors of genomic divergence

To dissect the effects of IBD, IBE, and isolation by river, we used multivariate logistic regression and commonality analysis (*43*). Because we were interested in fine-scale patterns of differentiation, we quantified pairwise genomic divergence among samples in each species using t-SNE (*39*) implemented in the iPyrad API analysis tools. t-SNE is a machine learning dimensionality reduction algorithm that decomposes high-dimensionality data into two components for more intuitive quantification and visualization and is capable of detecting subtle characteristics of datasets (*39*). First, we decomposed the data using PCA (as above) and then ran t-SNE on the PCA output (see above) to quantify the total genomic separation of samples across PC space.

However, t-SNE results are sensitive to two input parameters: "perplexity" (a parameter representing an approximate estimate of the number of neighboring points per cluster) and the starting seed (*39*). Although these values do not typically influence the general patterns recovered by t-SNE, no two t-SNE runs that differ in seed and perplexity will produce identical results. To account for variance among t-SNE runs, we performed 10,000 t-SNE replicates, randomly choosing perplexity values (integers between three and eight) and starting seeds. We then used the average pairwise Euclidean distances between samples in t-SNE space as a measure of genomic divergence. We also compared these results to those based on a coarser measure of divergence, pairwise genetic distance (d_{xy}).

We measured geographic distance by taking the least cost-path distance between sample localities based on environmental niche models (see Supplementary Materials and Methods). This method provides a metric of geographic distance that reflects the most likely dispersal paths based on habitat suitability on the landscape. The least cost-path distances were calculated using the R package GDISTANCE (*75*). To measure environmental disparity, we extracted climatic data from 19 BioClim variables (*76*) for all sample localities and used PCA to summarize the climatic conditions at each locality. We then calculated the Euclidean distance between all samples in this 10-dimensional climatic PC space.

Last, to test the assumption that rivers are barriers, we generated a pairwise matrix of individuals, where sample pairs were scored as either 0 (not separated by a river) or 1 (separated by a river). We specifically tested the seven focal river barriers corresponding to the boundaries of the eight a priori defined populations (Purus, Madeira, Jiparaná, Roosevelt, Aripuanã, Sucunduri, and Tapajós rivers). Although not all rivers should be considered equal, we discretized these barriers to conservatively test for their overall effects on genomic divergence. Although other potentially important riverine barriers occur in the region, our sampling is strongest across these seven rivers, and we therefore did not test other rivers (e.g., the Juruá River).

We then modeled genomic divergence as a function of these three spatial variables (dispersal distance, environmental disparity, and rivers). Ordinary least squares (OLS) linear regression models are commonly applied in landscape genetics, but they assume that the model residuals are normally distributed. We plotted divergence data for each species and found it to be multimodal without exception, thus violating the assumptions of OLS regression. To address this problem, following Prunier *et al.* (*43*), we transformed genomic divergences into binary variables of zero (i.e., failure to diverge) or one (successful divergence). To define our threshold for this transformation, a kernel density with an adjustment of 0.25 was used to estimate the boundaries of each mode in the standardized divergence data. Divergences were standardized using a z transformation (subtract the mean and divide by SD). Any values falling within the first mode (i.e., before the kernel density begins to increase for a second time; figs. S5 and S6) were scored as 0 (failed divergences). Those that fell above the first mode (i.e., after the kernel density begins to increase for a second time) were scored as 1 (successful divergences). Then, logistic regression was performed using the glm function with a logit link in R 4.0.3 to predict the likelihood of a success (i.e., the probability that $Y = 1$) given the three predictor variables (dispersal distance, environmental disparity, and rivers) (*43*). To assess the overall fit of each model, we computed pseudo-R^2 using Nagelkerke's index using the R package fmsb with a range from zero to one (see also the Supplementary Materials).

To evaluate the relative contributions of each variable while controlling for multicollinearity among predictors, we also performed logistic commonality analysis using the cc4log function available in the work of Roberts and Nimon (*77*). Commonality analysis is a variance partitioning approach that determines the relative contributions of a set of independent variables on a dependent variable while accounting for nonindependence among predictors. This helps us to pinpoint the location and extent of multicollinearity among variables. To do this, the multivariate logistic regression model is decomposed into its unique and common contributions. The unique contribution of a given predictor represents the proportion of the pseudo-R^2 (i.e., the proportion of total variance in genomic divergence explained by the multivariate logistic regression model) that is explained solely by that predictor. Common contributions represent the proportions of the total pseudo-R^2 that are explained by that predictor in combination with other predictors. The total contribution of each predictor, the commonality coefficient, is thus quantified irrespective of any nonindependence among predictors. To do this, we adapted R scripts from Prunier *et al.* (*43*) and Seeholzer and Brumfield (*78*). We also z-transformed all predictors to generate comparable beta weights (β) and odd ratios (ψ) (*43*). Last, we computed 95% confidence intervals around for commonality coefficients by performing 1000 bootstrap replicates on random selections of 90% of samples without replacement (see the Supplementary Materials).

Phylogenomic species trees

We estimated the historical relationships among a priori populations using ASTRAL 5.7.3 (*41*). ASTRAL estimates the species tree from a set of unrooted gene trees under the multispecies coalescent model, with an assumption of no gene flow among species. To assess the robustness of the inferred population relationships, we also applied 100 bootstraps, subsampling gene trees only, using the --gene-only flag. Gene trees were generated for all loci greater than 400 bp

in length. To reduce potential noise from gene tree estimation error, we then applied a filtering algorithm that identifies outlier loci (loci deviating from clock likeness expectations across the genome) (*56*). Species trees were rooted on the basis of the reference genome sequences for each species group (see Supplementary Materials and Methods).

Tests of introgression

To examine the evolutionary relationships within each species while relaxing the assumption of no gene flow, we additionally applied Bayesian phylogenomic network analysis using the MCMC_GT algorithm implemented in PhyloNet (*44*). This algorithm uses a reverse-jump MCMC (rjMCMC) to sample the posterior distribution of phylogenetic networks under an MSNC model. The MSNC models genome evolution as a network (as opposed to bifurcating tree), accounting for both incomplete lineage sorting and interlineage gene flow (reticulation). We used the same set of gene trees filtered under the above criteria to estimate the network for each species. We ran the rjMCMC for 5×10^7 generations with a burn-in of 5×10^6, sampling every 10^5 generations, using the pseudo-likelihood calculation, and allowing a maximum of two reticulate nodes per network (the rjMCMC will thus test networks with zero, one, and two reticulations only). The network topology with the highest PP is chosen as the most credible network topology.

Last, we used TreeMix 1.13 (*45*) to estimate the maximum likelihood population graph in the presence of gene flow by attaching migration edges (inferred shared ancestry due to genetic exchange) to a tree of bifurcating populations. Migration edges are assigned migration weights, which are related to the proportion of alleles in a population that are derived from migration. To examine the sensitivity of TreeMix output to missing data, we first ran TreeMix on subsamples of 50, 60, 70, 80, and 90% missing data with one migration edge ($m = 1$). We then examined the model fit for varying values of m ($m = 0$ to 3), where m represents the number of migration edges in the model (zero represents a pure isolation model). To do so, we performed 250 TreeMix replicates, randomly choosing missing data thresholds between 50% and 95% and quantifying the likelihood of the model and averaging across all replicates. This was repeated for each value of m.

Because unstructured populations may experience high gene flow, for both PhyloNet and TreeMix, we assigned individuals to populations based on their assignments in STRUCTURE. However, because STRUCTURE analyses resulted in underestimation of population structure for *Thamnophilus* and *Phlegopsis* when compared with PCA and previous work (*8*, *24*), we split one of the population assignments in two based on PCA results with the goal of better understanding spatial patterns of isolation and reticulation in these groups (for additional details, see Supplementary Materials and Methods).

Demographic modeling

To estimate divergence times and effective population sizes in the presence of gene flow, we applied a Bayesian approach using Generalized Phylogenetic Coalescent Sampler (G-PhoCS) (*47*). G-PhoCS integrates full likelihood computation across all possible gametic phasings based on unphased loci and a predefined demographic model to estimate mutation-scaled effective population sizes (θ) and divergence times (τ) for all populations. The software also allows estimation of continuous gene flow between sets of current and ancestral populations. We constructed demographic models for each species group based on the results from PhyloNet. Specifically, reticulate edges in PhyloNet with higher inheritance probabilities (>0.5) were treated as population divergences, whereas the edges with lower probabilities (<0.5) were treated as migration edges. We allowed for all possible migration edges based on both PhyloNet and TreeMix results. We applied priors on root τ ($\alpha = 3.0$ and $\beta = 1000$) and θ ($\alpha = 5.0$ and $\beta = 1000$), migration ($\alpha = 1.2$ and $\beta = 0.01$), and divergence (τ: $\alpha = 1.0$ and $\beta = 50{,}000$; θ: $\alpha = 5.0$ and $\beta = 1000$) for each population. We then ran the MCMC for 5×10^5 iterations after a burn-in of 10%, and sampling every 10 iterations. To convert τ and θ outputs to absolute divergence times (T) and effective population sizes (N_e), respectively, we used the formulas $N_e = \theta/4\mu$ and $T = \tau G/\mu$, where μ is the mutation rate in substitutions per site per generation, and G is the generation time in years (for additional details, see Supplementary Materials and Methods).

SUPPLEMENTARY MATERIALS

Supplementary material for this article is available at https://science.org/doi/10.1126/sciadv.abn1099

View/request a protocol for this paper from *Bio-protocol*.

REFERENCES AND NOTES

1. J. S. Albert, J. M. Craig, V. A. Tagliacollo, P. Petry, Upland and lowland fishes: A test of the river capture hypothesis. *Mountains Clim. Biodiver.*, 273–294 (2018).
2. J. Cracraft, C. Camila Ribas, F. M. d'Horta, J. Bates, R. P. Almeida, A. Aleixo, J. P. Boubli, K. E. Campbell, F. W. Cruz, M. Ferreira, S. C. Fritz, C. H. Grohmann, E. M. Latrubesse, L. G. Lohmann, L. J. Musher, A. Nogueira, A. O. Sawakuchi, P. Baker, in *Neotropical Diversification: Patterns and Processes*, V. Rull, A. C. Carnaval, Eds. (Springer International Publishing, 2020), pp. 225–244.
3. C. C. Ribas, A. Aleixo, A. C. R. Nogueira, C. Y. Miyaki, J. Cracraft, A palaeobiogeographic model for biotic diversification within Amazonia over the past three million years. *Proc. Biol. Sci.* **279**, 681–689 (2012).
4. J. Cracraft, Historical biogeography and patterns of differentiation within the South American avifauna: Areas of endemism. *Ornithol. Monogr.* **1985**, 49–84 (1985).
5. F. C. P. Dagosta, M. De Pinna, The fishes of the amazon: Distribution and biogeographical patterns, with a comprehensive list of species. *Bull. Am. Mus. Nat. Hist.* **2019**, 1 (2019).
6. J. S. Albert, P. Petry, R. E. Reis, Major biogeographic and phylogenetic patterns. *Historical Biogeogr. Neotropical Freshwater Fishes.* **1**, 21–57 (2011).
7. B. T. Smith, J. E. McCormack, A. M. Cuervo, M. J. Hickerson, A. Aleixo, C. D. Cadena, J. Pérez-Emán, C. W. Burney, X. Xie, M. G. Harvey, B. C. Faircloth, T. C. Glenn, E. P. Derryberry, J. Prejean, S. Fields, R. T. Brumfield, The drivers of tropical speciation. *Nature* **515**, 406–409 (2014).
8. S. M. Silva, A. T. Peterson, L. Carneiro, T. C. T. Burlamaqui, C. C. Ribas, T. Sousa-Neves, L. S. Miranda, A. M. Fernandes, F. M. d'Horta, L. E. Araújo-Silva, R. Batista, C. H. M. M. Bandeira, S. M. Dantas, M. Ferreira, D. M. Martins, J. Oliveira, T. C. Rocha, C. H. Sardelli, G. Thom, P. S. Rêgo, M. P. Santos, F. Sequeira, M. Vallinoto, A. Aleixo, A dynamic continental moisture gradient drove Amazonian bird diversification. *Sci. Adv.* **5**, eaat5752 (2019).
9. G. Thom, A. T. Xue, A. O. Sawakuchi, C. C. Ribas, M. J. Hickerson, A. Aleixo, C. Miyaki, Quaternary climate changes as speciation drivers in the Amazon floodplains. *Sci. Adv.* **6**, eaax4718 (2020).
10. C. Burney, R. Brumfield, Ecology predicts levels of genetic differentiation in neotropical birds. *Am. Nat.* **174**, 358–368 (2009).
11. S. Claramunt, E. P. Derryberry, J. V. Remsen Jr., R. T. Brumfield, High dispersal ability inhibits speciation in a continental radiation of passerine birds. *Proc. Biol. Sci.* **279**, 1567–1574 (2012).
12. N. M. A. Crouch, J. M. G. Capurucho, S. J. Hackett, J. M. Bates, Evaluating the contribution of dispersal to community structure in Neotropical passerine birds. *Ecography* **42**, 390–399 (2019).
13. K. Ruokolainen, G. M. Moulatlet, G. Zuquim, C. Hoorn, H. Tuomisto, Geologically recent rearrangements in central Amazonian river network and their importance for the riverine barrier hypothesis. *Front. Biogeogr.* **11**, 5596q2g4 (2019).
14. C. C. Mason, B. W. Romans, D. F. Stockli, R. W. Mapes, A. Fildani, Detrital zircons reveal sea-level and hydroclimate controls on Amazon River to deep-sea fan sediment transfer. *Geology* **47**, 563–567 (2019).
15. L. J. Musher, P. J. Galante, G. Thom, J. W. Huntley, M. E. Blair, Shifting ecosystem connectivity during the Pleistocene drove diversification and gene-flow in a species complex of Neotropical birds (Tityridae: Pachyramphus). *J. Biogeogr.* **66**, 167 (2020).

16. J. T. Weir, M. S. Faccio, P. Pulido-Santacruz, A. O. Barrera-Guzmán, A. Aleixo, Hybridization in headwater regions, and the role of rivers as drivers of speciation in Amazonian birds. *Evolution* **69**, 1823–1834 (2015).
17. F. N. Pupim, A. O. Sawakuchi, R. P. Almeida, C. C. Ribas, A. K. Kern, G. A. Hartmann, C. M. Chiessi, L. N. Tamura, T. D. Mineli, J. F. Savian, C. H. Grohmann, D. J. Bertassoli, A. G. Stern, F. W. Cruz, J. Cracraft, Chronology of Terra Firme formation in Amazonian lowlands reveals a dynamic Quaternary landscape. *Quat. Sci. Rev.* **210**, 154–163 (2019).
18. J. V. Peñalba, L. Joseph, C. Moritz, Current geography masks dynamic history of gene flow during speciation in northern Australian birds. *Mol. Ecol.* **28**, 630–643 (2019).
19. D. F. Rossetti, The role of tectonics in the late Quaternary evolution of Brazil's Amazonian landscape. *Earth Sci. Rev.* **139**, 362–389 (2014).
20. J. S. Albert, M. J. Bernt, A. H. Fronk, J. P. Fontenelle, S. L. Kuznar, N. R. Lovejoy, Late Neogene megariver captures and the Great Amazonian biotic interchange. *Glob. Planet. Change* **205**, 103554 (2021).
21. B. T. Smith, G. F. Seeholzer, M. G. Harvey, A. M. Cuervo, R. T. Brumfield, A latitudinal phylogeographic diversity gradient in birds. *PLoS Biol.* **15**, e2001073 (2017).
22. M. G. Harvey, G. F. Seeholzer, B. T. Smith, D. L. Rabosky, A. M. Cuervo, R. T. Brumfield, Positive association between population genetic differentiation and speciation rates in New World birds. *Proc. Natl. Acad. Sci. U.S.A.* **114**, 6328–6333 (2017).
23. M. Ferreira, A. Aleixo, C. C. Ribas, M. P. D. Santos, Biogeography of the Neotropical genus *Malacoptila* (Aves: Bucconidae): The influence of the Andean orogeny, Amazonian drainage evolution and palaeoclimate. *J. Biogeogr.* **44**, 748–759 (2017).
24. G. Thom, A. Aleixo, Cryptic speciation in the white-shouldered antshrike (*Thamnophilus aethiops*, Aves–Thamnophilidae): The tale of a transcontinental radiation across rivers in lowland Amazonia and the northeastern Atlantic Forest. *Mol. Phylogenet. Evol.* **82**, 95–110 (2015).
25. M. L. Isler, P. R. Isler, B. M. Whitney, Species limits in antbirds (Thamnophilidae): The warbling antbird (*Hypocnemis Cantator*) complex. *Auk* **124**, 11–28 (2007).
26. A. M. Fernandes, Fine-scale endemism of Amazonian birds in a threatened landscape. *Biodivers. Conserv.* **22**, 2683–2694 (2013).
27. J. C. Buckner, J. W. Lynch Alfaro, A. B. Rylands, M. E. Alfaro, Biogeography of the marmosets and tamarins (Callitrichidae). *Mol. Phylogenet. Evol.* **82**, 413–425 (2015).
28. H. Byrne, J. W. Lynch Alfaro, I. Sampaio, I. Farias, H. Schneider, T. Hrbek, J. P. Boubli, Titi monkey biogeography: Parallel Pleistocene spread by *Plecturocebus* and *Cheracebus* into a post-Pebas Western Amazon. *Zool. Scr.* **47**, 499–517 (2018).
29. M. T. Rodrigues, M. Cohn-Haft, Are Amazonia Rivers biogeographic barriers for lizards? A study on the geographic variation of the spectacled lizard *Leposoma osvaldoi* Avila-Pires (Squamata, Gymnophthalmidae). *J. Herpetol.* **47**, 511–519 (2013).
30. J. P. W. Hall, D. J. Harvey, The phylogeography of Amazonia revisited: New evidence from riodinid butterflies. *Evolution* **56**, 1489–1497 (2002).
31. T. C. Bicudo, V. Sacek, R. P. de Almeida, J. M. Bates, C. C. Ribas, Andean tectonics and mantle dynamics as a pervasive influence on amazonian ecosystem. *Sci. Rep.* **9**, 16879 (2019).
32. P. Bishop, Drainage rearrangement by river capture, beheading and diversion. *Progr. Phys. Geogr. Earth Environ.* **19**, 449–473 (1995).
33. D. M. Arruda, C. E. G. R. Schaefer, R. S. Fonseca, R. R. C. Solar, E. I. Fernandes-Filho, Vegetation cover of Brazil in the last 21 ka: New insights into the Amazonian refugia and Pleistocenic arc hypotheses. *Glob. Ecol. Biogeogr.* **27**, 47–56 (2018).
34. H. Tuomisto, J. Van Doninck, K. Ruokolainen, G. M. Moulatlet, F. O. G. Figueiredo, A. Sirén, G. Cárdenas, S. Lehtonen, G. Zuquim, Discovering floristic and geoecological gradients across Amazonia. *J. Biogeogr.* **46**, 1734–1748 (2019).
35. C. Gascon, J. R. Malcolm, J. L. Patton, M. N. da Silva, J. P. Bogart, S. C. Lougheed, C. A. Peres, S. Neckel, P. T. Boag, Riverine barriers and the geographic distribution of Amazonian species. *Proc. Natl. Acad. Sci. U.S.A.* **97**, 13672–13677 (2000).
36. D. A. Marques, J. I. Meier, O. Seehausen, A combinatorial view on speciation and adaptive radiation. *Trends Ecol. Evol.* **34**, 531–544 (2019).
37. S. Wright, Isolation by distance. *Genetics* **28**, 114–138 (1943).
38. I. J. Wang, G. S. Bradburd, Isolation by environment. *Mol. Ecol.* **23**, 5649–5662 (2014).
39. W. Li, J. E. Cerise, Y. Yang, H. Han, Application of t-SNE to human genetic data. *J. Bioinform. Comput. Biol.* **15**, 1750017 (2017).
40. M. J. Hubisz, D. Falush, M. Stephens, J. K. Pritchard, Inferring weak population structure with the assistance of sample group information. *Mol. Ecol. Resour.* **9**, 1322–1332 (2009).
41. C. Zhang, M. Rabiee, E. Sayyari, S. Mirarab, ASTRAL-III: Polynomial time species tree reconstruction from partially resolved gene trees. *BMC Bioinform.* **19**, 153 (2018).
42. D. Petkova, J. Novembre, M. Stephens, Visualizing spatial population structure with estimated effective migration surfaces. *Nat. Genet.* **48**, 94–100 (2016).
43. J. G. Prunier, M. Colyn, X. Legendre, K. F. Nimon, M. C. Flamand, Multicollinearity in spatial genetics: Separating the wheat from the chaff using commonality analyses. *Mol. Ecol.* **24**, 263–283 (2015).
44. D. Wen, Y. Yu, L. Nakhleh, Bayesian inference of reticulate phylogenies under the multispecies network coalescent. *PLOS Genet.* **12**, e1006006 (2016).
45. J. K. Pickrell, J. K. Pritchard, Inference of population splits and mixtures from genome-wide allele frequency data. *PLOS Genet.* **8**, e1002967 (2012).
46. A. O. Barrera-Guzmán, A. Aleixo, M. D. Shawkey, J. T. Weir, Hybrid speciation leads to novel male secondary sexual ornamentation of an Amazonian bird. *Proc. Natl. Acad. Sci. U.S.A.* **115**, E218–E225 (2018).
47. I. Gronau, M. J. Hubisz, B. Gulko, C. G. Danko, A. Siepel, Bayesian inference of ancient human demography from individual genome sequences. *Nat. Genet.* **43**, 1031–1034 (2011).
48. J. Mallet, Hybrid speciation. *Nature* **446**, 279–283 (2007).
49. G. Thom, F. R. D. Amaral, M. J. Hickerson, A. Aleixo, L. E. Araujo-Silva, C. C. Ribas, E. Choueri, C. Y. Miyaki, Phenotypic and genetic structure support gene flow generating gene tree discordances in an Amazonian floodplain endemic species. *Syst. Biol.* **67**, 700–718 (2018).
50. J. Ebersbach, A. Posso-Terranova, S. Bogdanowicz, M. Gómez-Díaz, M. X. García-González, W. Bolívar-García, J. Andrés, Complex patterns of differentiation and gene flow underly the divergence of aposematic phenotypes in Oophaga poison frogs. *Mol. Ecol.* **29**, 1944–1956 (2020).
51. A. Springer, Z. Gompert, Species collisions, admixture, and the genesis of biodiversity in poison frogs. *Mol. Ecol.* **29**, 1937–1940 (2020).
52. P. A. Maier, A. G. Vandergast, S. M. Ostoja, A. Aguilar, A. J. Bohonak, Pleistocene glacial cycles drove lineage diversification and fusion in the Yosemite toad (Anaxyrus canorus). *Evolution* **73**, 2476–2496 (2019).
53. F. E. Rheindt, M. K. Fujita, P. R. Wilton, S. V. Edwards, Introgression and phenotypic assimilation in *Zimmerius* flycatchers (Tyrannidae): Population genetic and phylogenetic inferences from genome-wide SNPs. *Syst. Biol.* **63**, 134–152 (2014).
54. R. G. Gillespie, J. Lim, A. J. Rominger, The theory of evolutionary biogeography, in *The Theory of Evolution: Principles, Concepts, and Assumptions*, S. M. Scheiner, D. P. Mindell, Eds. (University of Chicago Press, 2020), pp. 319–337.
55. J. S. Albert, D. R. Schoolmaster Jr., V. Tagliacollo, S. M. Duke-Sylvester, Barrier displacement on a neutral landscape: Toward a theory of continental biogeography. *Syst. Biol.* **66**, 167–182 (2017).
56. L. J. Musher, M. Ferreira, A. L. Auerbach, J. Cracraft, Why is Amazonia a 'source' of biodiversity? Climate-mediated dispersal and synchronous speciation across the Andes in an avian group (Tityrinae). *Proc. Roy. Soc. B* **286**, 20182343 (2019).
57. R. P. Moore, W. D. Robinson, I. J. Lovette, T. R. Robinson, Experimental evidence for extreme dispersal limitation in tropical forest birds. *Ecol. Lett.* **11**, 960–968 (2008).
58. B. C. Weeks, S. Claramunt, J. Cracraft, Integrating systematics and biogeography to disentangle the roles of history and ecology in biotic assembly. *J. Biogeogr.* **43**, 1546–1559 (2016).
59. J. Fjeldså, Geographical patterns for relict and young species of birds in Africa and South America and implications for conservation priorities. *Biodivers. Conserv.* **3**, 207–226 (1994).
60. S. Claramunt, J. Cracraft, A new time tree reveals Earth history's imprint on the evolution of modern birds. *Sci. Adv.* **1**, e1501005 (2015).
61. G. Del-Rio, M. A. Rego, B. M. Whitney, F. Schunck, L. F. Silveira, B. C. Faircloth, R. T. Brumfield, Displaced clines in an avian hybrid zone (Thamnophilidae: *Rhegmatorhina*) within an Amazonian interfluve. *Evolution* 10.1111/evo.14377, (2021).
62. A. B. Rylands, A. F. Coimbra-Filho, R. A. Mittermeier, in *The Smallest Anthropoids: The Marmoset/Callimico Radiation*, S. M. Ford, L. M. Porter, L. C. Davis, Eds. (Springer US, 2009), pp. 25–61.
63. H. Byrne, R. Costa-Araújo, I. P. Farias, M. N. F. da Silva, M. Messias, T. Hrbek, J. P. Boubli, Uncertainty regarding species delimitation, geographic distribution, and the evolutionary history of South-Central Amazonian titi monkey species (*Plecturocebus*, Pitheciidae). *Int. J. Primatol.* 10.1007/s10764-021-00249-9, (2021).
64. P. Hovenkamp, Vicariance events, not areas, should be used in biogeographical analysis. *Cladistics* **13**, 67–79 (1997).
65. L. N. Naka, R. T. Brumfield, The dual role of Amazonian rivers in the generation and maintenance of avian diversity. *Sci. Adv.* **4**, eaar8575 (2018).
66. J. S. de Jesus, F. do N. Pupim, A. O. Sawakuchi, L. B. Felipe, Geomorphology of fluvial deposits in the middle Tocantins River, eastern Amazon. *J. Maps* **16**, 710–723 (2020).
67. E. M. Fonseca, A. A. Garda, E. F. Oliveira, F. Camurugi, F. de M. Magalhães, F. M. Lanna, J. P. Zurano, R. Marques, M. Vences, M. Gehara, The riverine thruway hypothesis: Rivers as a key mediator of gene flow for the aquatic paradoxical frog *Pseudis tocantins* (Anura, Hylidae). *Landsc. Ecol.* **36**, 3049–3060 (2021).
68. J. Cracraft, R. O. Prum, Patterns and processes of diversification: Speciation and historical congruence in some neotropical birds. *Evolution* **42**, 603–620 (1988).
69. C. N. Jenkins, S. L. Pimm, L. N. Joppa, Global patterns of terrestrial vertebrate diversity and conservation. *Proc. Natl. Acad. Sci. U.S.A.* **110**, E2602–E2610 (2013).
70. Á. A. Cronemberger, A. Aleixo, E. K. Mikkelsen, J. T. Weir, Postzygotic isolation drives genomic speciation between highly cryptic Hypocnemis antbirds from Amazonia. *Evolution* **74**, 2512–2525 (2020).

71. L. Ferrante, P. M. Fearnside, The Amazon: Biofuels plan will drive deforestation. *Nature* **577**, 170 (2020).
72. V. H. F. Gomes, I. C. G. Vieira, R. P. Salomão, H. ter Steege, Amazonian tree species threatened by deforestation and climate change. *Nat. Clim. Chang.* **9**, 547–553 (2019).
73. P. M. Brando, B. Soares-Filho, L. Rodrigues, A. Assunção, D. Morton, D. Tuchschneider, E. C. M. Fernandes, M. N. Macedo, U. Oliveira, M. T. Coe, The gathering firestorm in southern Amazonia. *Sci. Adv.* **6**, eaay1632 (2020).
74. D. A. R. Eaton, I. Overcast, ipyrad: Interactive assembly and analysis of RADseq datasets. *Bioinformatics* **36**, 2592–2594 (2016).
75. J. van Etten, R package gdistance: Distances and routes on geographical grids. *J. Stat. Software* **76**, 1–21 (2017).
76. R. J. Hijmans, S. E. Cameron, J. L. Parra, P. G. Jones, A. Jarvis, Very high resolution interpolated climate surfaces for global land areas. *Int. J. Climatol.* **25**, 1965–1978 (2005).
77. J. K. Roberts, K. Nimon, in *Annual Meeting of the Southwest Educational Research Association, New Orleans* (2012).
78. G. F. Seeholzer, R. T. Brumfield, Isolation by distance, not incipient ecological speciation, explains genetic differentiation in an Andean songbird (Aves: Furnariidae: Cranioleuca antisiensis, line-cheeked spinetail) despite near threefold body size change across an environmental gradient. *Mol. Ecol.* **27**, 279–296 (2018).
79. K.-P. Koepfli, B. Paten; Genome 10K Community of Scientists, S. J. O'Brien, The Genome 10K Project: A way forward. *Annu. Rev. Anim. Biosci.* **3**, 57–111 (2015).
80. L. A. Coelho, L. J. Musher, J. Cracraft, A multireference-based whole genome assembly for the obligate ant-following antbird, *Rhegmatorhina melanosticta* (Thamnophilidae). *Diversity* **11**, 144 (2019).
81. H. Li, R. Durbin, Fast and accurate short read alignment with Burrows-Wheeler transform. *Bioinformatics* **25**, 1754–1760 (2009).
82. M. Jakobsson, N. A. Rosenberg, CLUMPP: A cluster matching and permutation program for dealing with label switching and multimodality in analysis of population structure. *Bioinformatics* **23**, 1801–1806 (2007).
83. G. Evanno, S. Regnaut, J. Goudet, Detecting the number of clusters of individuals using the software STRUCTURE: A simulation study. *Mol. Ecol.* **14**, 2611–2620 (2005).
84. B. Pfeifer, U. Wittelsbürger, S. E. Ramos-Onsins, M. J. Lercher, PopGenome: An efficient Swiss army knife for population genomic analyses in R. *Mol. Biol. Evol.* **31**, 1929–1936 (2014).
85. M. E. Aiello-Lammens, R. A. Boria, A. Radosavljevic, B. Vilela, R. P. Anderson, spThin: An R package for spatial thinning of species occurrence records for use in ecological niche models. *Ecography* **38**, 541–545 (2015).
86. R. Muscarella, P. J. Galante, M. Soley-Guardia, R. A. Boria, J. M. Kass, M. Uriarte, R. P. Anderson, ENMeval: An R package for conducting spatially independent evaluations and estimating optimal model complexity for Maxent ecological niche models. *Methods Ecol. Evol.* **5**, 1198–1205 (2014).
87. S. J. Phillips, R. P. Anderson, R. E. Schapire, Maximum entropy modeling of species geographic distributions. *Ecol. Model.* **190**, 231–259 (2006).
88. M. Shcheglovitova, R. P. Anderson, Estimating optimal complexity for ecological niche models: A jackknife approach for species with small sample sizes. *Ecol. Model.* **269**, 9–17 (2013).
89. S. Mirarab, R. Reaz, M. S. Bayzid, T. Zimmermann, M. S. Swenson, T. Warnow, ASTRAL: Genome-scale coalescent-based species tree estimation. *Bioinformatics* **30**, i541–i548 (2014).
90. A. Stamatakis, RAxML version 8: A tool for phylogenetic analysis and post-analysis of large phylogenies. *Bioinformatics* **30**, 1312–1313 (2014).
91. E. D. Jarvis, S. Mirarab, A. J. Aberer, B. Li, P. Houde, C. Li, S. Y. W. Ho, B. C. Faircloth, B. Nabholz, J. T. Howard, A. Suh, C. C. Weber, R. R. da Fonseca, J. Li, F. Zhang, H. Li, L. Zhou, N. Narula, L. Liu, G. Ganapathy, B. Boussau, M. S. Bayzid, V. Zavidovych, S. Subramanian, T. Gabaldón, S. Capella-Gutiérrez, J. Huerta-Cepas, B. Rekepalli, K. Munch, M. Schierup, B. Lindow, W. C. Warren, D. Ray, R. E. Green, M. W. Bruford, X. Zhan, A. Dixon, S. Li, N. Li, Y. Huang, E. P. Derryberry, M. F. Bertelsen, F. H. Sheldon, R. T. Brumfield, C. V. Mello, P. V. Lovell, M. Wirthlin, M. P. C. Schneider, F. Prosdocimi, J. A. Samaniego, A. M. V. Velazquez, A. Alfaro-Núñez, P. F. Campos, B. Petersen, T. Sicheritz-Ponten, A. Pas, T. Bailey, P. Scofield, M. Bunce, D. M. Lambert, Q. Zhou, P. Perelman, A. C. Driskell, B. Shapiro, Z. Xiong, Y. Zeng, S. Liu, Z. Li, B. Liu, K. Wu, J. Xiao, X. Yinqi, Q. Zheng, Y. Zhang, H. Yang, J. Wang, L. Smeds, F. E. Rheindt, M. Braun, J. Fjeldsa, L. Orlando, F. K. Barker, K. A. Jønsson, W. Johnson, K.-P. Koepfli, S. O'Brien, D. Haussler, O. A. Ryder, C. Rahbek, E. Willerslev, G. R. Graves, T. C. Glenn, J. McCormack, D. Burt, H. Ellegren, P. Alström, S. V. Edwards, A. Stamatakis, D. P. Mindell, J. Cracraft, E. L. Braun, T. Warnow, W. Jun, M. T. P. Gilbert, G. Zhang, Whole-genome analyses resolve early branches in the tree of life of modern birds. *Science* **346**, 1320–1331 (2014).
92. K. Nadachowska-Brzyska, C. Li, L. Smeds, G. Zhang, H. Ellegren, Temporal dynamics of avian populations during pleistocene revealed by whole-genome sequences. *Curr. Biol.* **25**, 1375–1380 (2015).
93. L. Smeds, A. Qvarnström, H. Ellegren, Direct estimate of the rate of germline mutation in a bird. *Genome Res.* **26**, 1211–1218 (2016).
94. J. Cracraft, Species concepts and speciation analysis. *Curr. Ornithol.* **1983**, 159–187 (1983).
95. E. Mayr, *Systematics and the Origin of Species, from the Viewpoint of a Zoologist: With a New Introduction by the Author* (1942).
96. P. Pulido-Santacruz, A. Aleixo, J. T. Weir, Morphologically cryptic Amazonian bird species pairs exhibit strong postzygotic reproductive isolation. *Proc. Biol. Sci.* **285**, 20172081 (2018).
97. J. M. I. Barth, C. Gubili, M. Matschiner, O. K. Tørresen, S. Watanabe, B. Egger, Y.-S. Han, E. Feunteun, R. Sommaruga, R. Jehle, R. Schabetsberger, Stable species boundaries despite ten million years of hybridization in tropical eels. *Nat. Commun.* **11**, 1433 (2020).

Acknowledgments: We thank T. Chiodo, L. Audi, S. Gaughran, A. Caragiulo, J. Groth, P. Sweet, R. Batista, F. Lima, I. Jean, and L. Jean for advice and assistance at various stages of this work. We additionally thank E. Grifith, J. Merwin, K. Kuabara, A. Del Grosso, and J. Weckstein for helpful comments on a previous version of this manuscript. We are grateful for the thoughtful suggestions of three anonymous referees that greatly improved the quality of this manuscript. **Funding:** This work was funded, in part, by Richard Gilder Graduate Research Fellowship (to L.J.M.), The Linda Gormezano Memorial Fund research grant (to L.J.M.), The Society for Systematic Biologists graduate student research grant (to L.J.M.), and NSF/NASA Dimensions US-Biota-São Paulo grant 1241066 (to J.C.). **Author contributions:** Conceptualization: L.J.M. and J.C. Methodology: L.J.M., M.G., and B.T.S. Investigation: L.J.M., M.G., G.D.-R., M.R., G.T., and A.A. Visualization: L.J.M. and M.G. Supervision: J.C. and B.T.S. Writing—original draft: L.J.M. (primarily) and J.A. Writing—review and editing: All authors. **Competing interests:** The authors declare that they have no competing interests. **Data and materials availability:** All data necessary for replicating are available on Dryad at https://datadryad.org/stash/dataset/doi:10.5061/dryad.w3r2280rv. Additional data, code, and materials used for replicating the analyses presented here are available at https://github.com/lukemusher/Southern_Amazon_cophylogeography.

Submitted 16 November 2021
Accepted 22 February 2022
Published 8 April 2022
10.1126/sciadv.abn1099

River network rearrangements promote speciation in lowland Amazonian birds

Lukas J. MusherMelina GiakoumisJames AlbertGlaucia Del-RioMarco RegoGregory ThomAlexandre AleixoCamila C. RibasRobb T. BrumfieldBrian Tilston SmithJoel Cracraft

Sci. Adv., 8 (14), eabn1099. • DOI: 10.1126/sciadv.abn1099